

## Promote Scientific Research is Our Way to Serve the Community



### Characterizations of CdS Thin Film Prepared by Chemical Drop Method

Jamal M. Rzaij , Sameer O. Nawaf , Mohammed Gh. Hammed

Department of physics, College of Science , University of Anbar, Ramadi, Iraq

#### ARTICLE INFO.

##### Keywords:

Microwave; nanoparticles, CdS preparation, Characterization.

Name: Jamal M. Rzaij

E-mail:

Tel:

#### ABSTRACT

A simple technique has been utilized to grow cadmium sulfide (CdS) nano size. The obtained nanoparticles powder was formed as thin films by chemical drop method. The prepared samples were annealed at 200 °C then illustrated by XRD, UV-VIS spectrum, AFM images and some dielectric properties. The results indicated that high purity of Nano sized CdS was successfully obtained with hexagonal crystalline structure with particles size estimated to be 35nm using x-ray line broadening. The optical band gap of prepared and annealing thin films varied with the range (3.35 – 3.73) eV. The AFM results show homogenized grains after annealing at 200 °C with surface roughness of 3.83 nm. Best values of dielectric were obtained for annealing samples.

#### 1. Introduction

Semiconductors have gotten massive consideration in the previous decades because of their affected size dependent [1–4]. These materials have revealed admirable electronic and optical properties [5], and well chemical stability as compared to organic emitters [6,7]. Cadmium sulfide (CdS) ( $E_g = 2.42$  eV) has a great interest in field of heterojunction (HJ) solar cells and characterized by many techniques [8]. It is suitable also for applications like visible radiation sensor [9]. Polycrystalline CdS are widely popular as window material in several (HJ) solar cells such as CdS/CdTe, CdS/CuS [10] for their favorable optical properties. Recently, CdS nanoparticles have been produced by numerous approaches including [11] sol–gel process [12], solid-state reaction, screen printing, hydrothermal method, electro deposition , molecular beam epitaxial (MBE) , physical vapor deposition, microwave etc,. Microwave can be defined as an electromagnetic radiation with the wavelength range of one millimeter to meter and frequency range (0.3–300) GHz [13]. As a result of properties of internal and volumetric heating, A thermal gradient through microwave processing can be prevented providing a uniform environment for chemical reaction [14]. This technique has been effectively utilized for the organic and metal clusters synthesis and the preparation of a range of Nano sized inorganic materials [15]. Microwave heating

has the benefit of high-efficiency and fast formation of nanoparticles with a narrow size distribution comparing with conventional heating,. In case of thin films preparation, many approaches have been fabricated such as vacuum evaporation, molecular beam epitaxy, metal-organic vapor phase epitaxy, spray pyrolysis, chemical bath deposition etc. In this work, we used a chemical drop method, which is simple inexpensive and simple method for production of thin films. The CdS nanoparticles prepared by employed the microwave irradiation working at 20% power.

#### 2. Experimental

Chemicals of analytical grade were utilized as received without additional purification. Cadmium chloride ( $\text{CdCl}_2$ , 0.1M), and thiourea [ $\text{CS}(\text{NH}_2)_2$ , 0.1M], were dissolved in 100 ml of 30% Ethylene glycol [ $\text{C}_2\text{H}_6\text{O}_2$ ] after mix together in a reaction beaker. A domestic microwave oven (1100W/230V-50Hz) system for 20 min with power 20%, meaning that the microwave working in full power as pulse regime (each 30 s regime it works 6 s and does not works in 24 s.). At the end of reaction the precipitate was centrifuged, then washed several times with ethanol, then dried up at 60 °C in oven. Portion of the sample was ultrasonically by propanol for 2h, then the product ready for preparation thin films by dropping few drops on clean glass substrate and

leaved in air to dry. Two samples (one was prepared and the other annealing at 200 °C for 2h) were ready for distinguished by XRD (PW1840) model with radiation of (Cu-K $\alpha$ ) and wavelength of 0.154 nm. The sizes of the prepared sample were calculated by Debye–Scherer formula according to XRD peak broadening. (USB2000, Ocean Optics) double beam was used as UV-vis spectrometer with the range of (200-1100) nm. Digital Instruments of Nasoscope IIIa system in air was used to perform AFM images.

### 3. Results and Discussion

#### 3.1 XRD studies

X-ray diffraction (XRD) patterns of as synthesis given in Fig. 1. Analysis of the diffractogram indicated of the sample exhibit peaks centered at  $2\theta = 24.75^\circ, 26.50^\circ, 28.10^\circ$  and  $36.65^\circ$ , which correspond to hexagonal wurtzite phase structure of nanocrystals with highly three favorite orientations along (100),

(101) and (002) planes. The peaks are satisfactory agree with the standard (JCPDS) file No. 41-1049 with lattice parameters  $a=4.145 \text{ \AA}$  and  $c=6.714 \text{ \AA}$ . X-ray diffraction verifies the phase singularity of the synthesized material, for example, there is no extra noticed peak matching with their binary system. Broad diffraction peaks verify the monocrystalline characteristics of the particles and can be utilized to compute the average crystallite size ( $G_s$ ) using Scherrer's formula [16]:

$$G_s = \frac{0.9\lambda}{\beta \cos \theta}$$

Where  $\lambda$  is the wavelength of x-ray target,  $\beta$  is full width at half maximum (FWHM) and  $\theta$  is Bragg angle in radiant. The approximated crystallite size of the nanocrystals using Scherrer's formula was calculated to be about 35 nm.

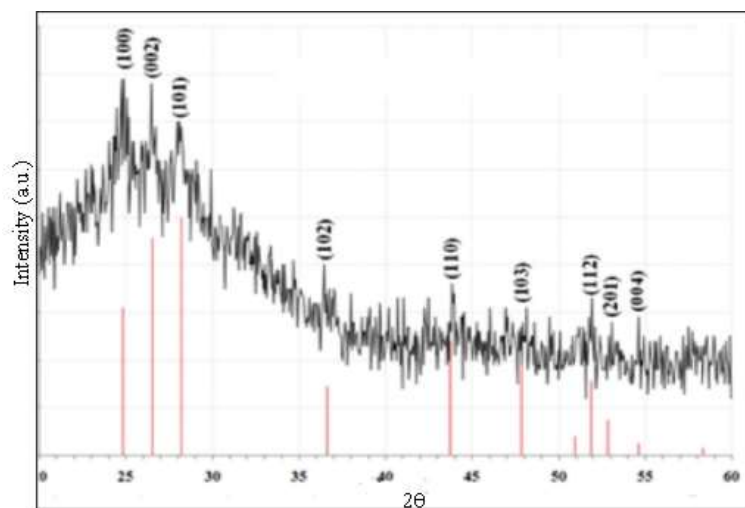


Figure 1: X-ray diffraction of CdS nanoparticles

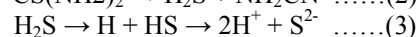
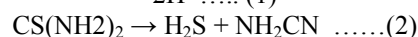
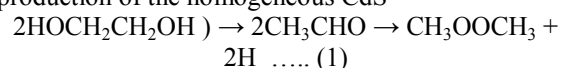
Table 1: comparative between experimental and standard peaks

$2\theta$ (Degree)	$d_{hkl}$ Exp. (Å)	FWHM	$G_s$ (Å)	$d_{hkl}$ Std. (Å)	hkl
24.75	3.594	0.62	163	3.586	(100)
26.50	3.361	0.66	150	3.360	(002)
28.10	3.173	0.70	140	3.164	(101)
36.65	2.450	0.72	138	2.452	(102)
43.85	2.063	0.80	124	2.071	(110)
48.15	1.888	0.80	126	1.900	(103)
51.90	1.760	0.70	151	1.763	(112)
53.05	1.725	0.70	152	1.733	(201)
54.60	1.679	0.86	118	1.679	(004)

#### 3.2. Reaction Mechanism

Ethylglycol was presented as a decreasing agent matching with the proposed mechanism by Wan et al.[17]. In case of synthesizing copper sulfide hollow spheres in ethylene glycol solvent, acetaldehyde can be manufactured by dehydration of ethylglycol at very high temperature, where the acetaldehyde gives a hydrogen atom and performance as a decreasing agent, as illustrated in Equation.1 [23]. In addition, thiourea is added into the reaction too. Thiourea

molecules give sulfur anions ( $S^{2-}$ ), in ethylglycol solution as in Equation.3 [26]. Therefore, CdS nano size is regularly formed by the competitive reaction between Thiourea molecules and sulfur ions  $Cd^{2+}$ . Similarly, perform as a surface stabilizer causing the production of the homogeneous CdS





### 3.3. UV-Vis Spectrum

Figure (2) shows the wavelength dependence transmittance of CdS samples in wavelength range of 300nm-1100nm. The optical transmittance of the CdS film produced at room temperature was approximately 20% above wavelength  $\approx 365\text{nm}$  while this value was increasing up to 60% when the sample was annealing at  $200^\circ\text{C}$  which may due to the stress relief increasing in crystallization and the stability of the film. This result of transmittance obeyed with the results of Hasnat [18] using spray pyrolyzed method and Hani et al.[19] Using chemical bath deposition method. Below 350nm, there is a clear drop in the value of transmittance of the thin film because of the high effective absorbance of the thin films in this range.

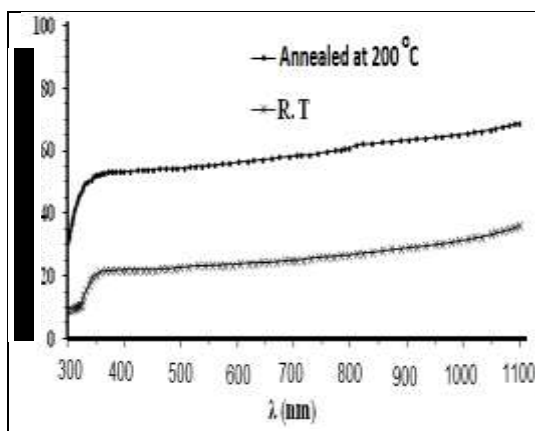


Figure 2: Relation between transmission and wavelength at UV-VIS region of CdS nanoparticles

### 3.4. Energy Band Gap

The energy band gap could be obtained from spectroscopy measurements [20]. We found the following results. Fig.3 display  $(\alpha h\nu)^2$  as a function of  $h\nu$ , where  $\alpha$  is the absorbent coefficient of the film. By plotting the figure between  $(\alpha h\nu)^2$  and photon energy ( $h\nu$ ) provides the value of direct energy band gap. The extrapolation of the straight line to  $(\alpha h\nu)^2$  gives the value of energy band gap. Two band gaps were recorded one at 3.35 eV for original prepared sample and the other at 3.73 eV after annealing at  $200^\circ\text{C}$ . Those results are greater than the value of bulk and thin film for CdS reported. This shift in energy band gap attributed to the structure of  $(\text{CdS})_n$  clusters ( $2 \leq n \leq 5$ ) as informed by [21] and they found the structure of CdS monomers and  $(\text{CdS})_n$  clusters shaped at the initial stages of  $(\text{Cd}^{+2}$  ions and  $\text{S}^{2-}$  ions) reaction as in Fig.4. They found the band gap at  $n=3$  was 3.69 eV and when  $n=4$  the band gap was 3.29 eV. That mean in our work the  $n$  have the values of 3 and 4. This results also in agreement with the results of Zeng [14].

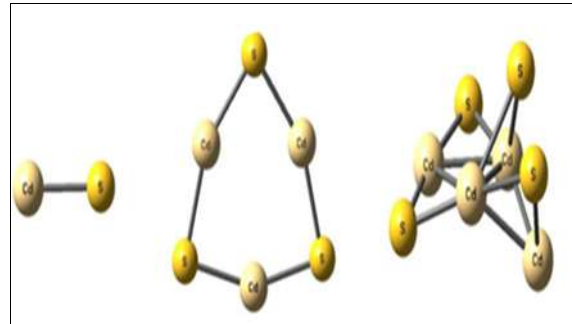


Figure 3: The relation between  $(\alpha h\nu)^2$  and  $h\nu$  for CdS nanoparticles.

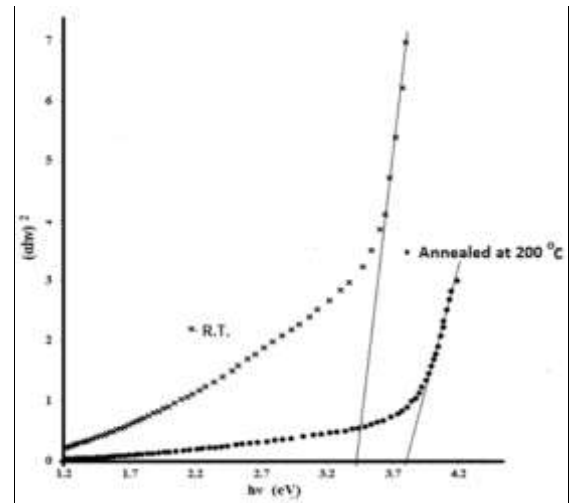


Figure 4: Coordination of  $(\text{CdS})_n$  cluster with  $n=1,3$  and 4[21]

### 3.5. Dielectric properties

Dielectric properties of real and imaginary parts of the dielectric constant were illustrated in Figures 5 and 6. The real part is dependable of reducing the speed of light in material while the imaginary part acts as absorb energy from electric field because of the dipole motion. It is quite clear the effect of temperature on the results. After 340 nm, the  $\epsilon_r$  value increases in case of original prepared sample and decreasing for annealing one. A good result was obtained for  $\epsilon_i$  values in case of annealing sample to give all the values below 1.

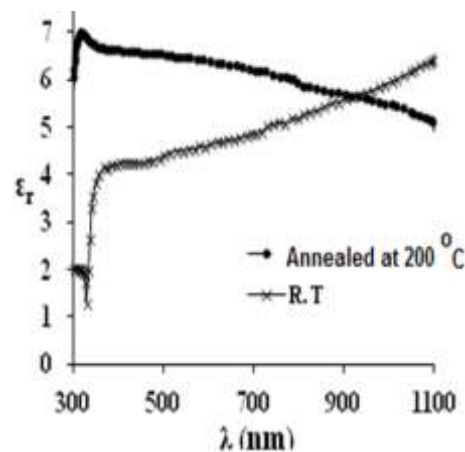


Figure 5: Behavior of  $\epsilon_r$  at UV-VIS region

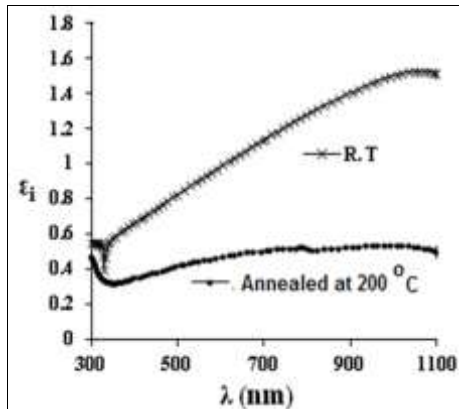


Figure 6: Behavior of  $\epsilon_i$  at UV-VIS region

### 3.6. Atomic force microscopy

Atomic force microscopy AFM has been utilized to analysis the surface morphology of the CdS films. The matching AFM image are showed in Fig.7-a related to room temperature. A weak crystalline are formed and does not indicate a high particular

structure and exhibits a low surface roughness 1.3 nm. As temperature increases, 200 °C , CdS film crystallization occurred then AFM images of the film grow up at a granulated structure, with low surface roughness 3.83 nm, Fig.7-b, comparing with literatures.

The images of the atomic force microscope, Fig.7-a, showed the presence of black point-like interspersed with the deposited atoms, which represent point defects that may be caused by the oxygen vacancy that accompanying the deposition process, same result with [24,25], or may represent impurities deposited on the surface during the preparation of films. Figure 7-b shows the disappearance of most those spots This may be due to the fact that the annealing process has greatly contributed to reducing the defects of oxygen vacancies and rearranging the atoms in crystalline form.

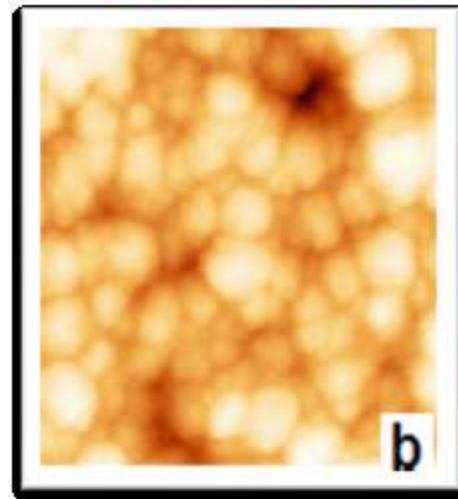
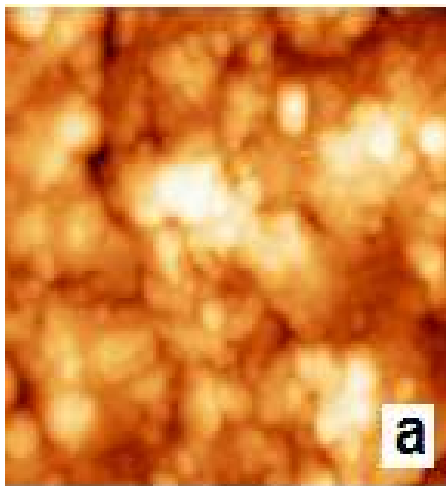


Figure 7: Evolution of the AFM images (a) at room temperature and (b) at 200 °C.

### Conclusions

We have shown that CdS prepared by microwave radiation can form thin films on glass substrates by chemical drop technique. Results of x-ray showed particles near 35 nm in size of uniform crystal shape structure after annealing. UV–VIS spectra observed that the transmission spectra shift towards shorter wavelength. Shift in energy gap attributed to the

### References

- [1] Banerjee, R.; Jayakrishnan, R. and Ayyub, P. (2000). Effect of the size-induced structural transformation on the band gap in CdS nanoparticles. *Journal of Physics: Condensed Matter. IOP Publishing*, **12(50)**:10647.
- [2] Dobson, K. D.; Fisher, I.; Hodes, G. and Cahen, D. (2000). Stability of CdTe/CdS thin-film solar cells. *Solar Energy Materials and Solar Cells. Elsevier*, **62(3)**:295–325.
- [3] Ferrer, E. et al.(2012). Turning “on” and “off” nucleation and growth: Microwave assisted synthesis

configuration of  $(\text{CdS})_n$  clusters ( $2 \leq n \leq 5$ ) for the structure of CdS monomers and  $(\text{CdS})_n$  clusters formed at the initial stages of the  $(\text{Cd}^{+2}$  ions and  $\text{S}^{-2}$  ions) reaction due to the microwave radiation time. Both  $\epsilon_r$  and  $\epsilon_i$  have a good result for annealing thin film. Atomic force microscopy shows a roughness value of 3.83 nm with high crystallization. All the results were obeyed the literature data.

- of CdS clusters and nanoparticles. *Materials Research Bulletin. Elsevier*, **47(11)**:3835–3843.
- [4] Hanaoka, T.; Teruoki, T.; Masahiro, K. and Katsuhiko, W. (2001). Size control of metastable ZnS particles in W/O microemulsion. *Bulletin of the Chemical Society of Japan. The Chemical Society of Japan*, **74(7)**:1349–1354.
- [5] Hochbaum, A. I. and Yang, P. (2009). Semiconductor nanowires for energy conversion. *Chemical reviews. ACS Publications*, **110(1)**:527–546.

- [6] Ishizumi, A. and Kanemitsu, Y. (2006). Luminescence Spectra and Dynamics of Mn-Doped CdS Core/Shell Nanocrystals. *Advanced Materials. Wiley Online Library*, **18(8)**:1083–1085.
- [7] Khallaf, H. et al. (2008). Investigation of aluminium and indium in situ doping of chemical bath deposited CdS thin films. *Journal of Physics D: Applied Physics. IOP Publishing*, **41(18)**:185304.
- [8] Liao, X.-H.; Chen, N.; Xu, S.; Yang, S. and Zhu, J. (2003). A microwave assisted heating method for the preparation of copper sulfide nanorods. *Journal of Crystal Growth. Elsevier*, **252(4)**:593–598.
- [9] Mohammed, A.; Ghazi, M. and Suhail, M. H. (2017). Some electrical properties of PVA : PEG / MnCl<sub>2</sub> thin film composites. *Iraqi Journal of Physics*, **15(33)**: 122–130.
- [10] Najim, J. A and Rozaiq, J. M. (2013). Effect Cd Doping on the Structural and Optical Properties of ZnO Thin Films. *International Letters of Chemistry, Physics and Astronomy*, **10(2)**:137–150.
- [11] Nawaf, S.; Rzaiz, J. M. and Motlak, M. (2018). Study on Au -Ni Core-Shell Nanowires for Optical Applications. *Indian Journal of Natural Sciences*, **8(47)**: 13591–13596.
- [12] Obaid, A. S.; Hammed, M. G. and Nawaf, S. O. (2018). Synthesis of ZnO Nanostructured using Simple Technique. *Indian Journal of Natural Sciences*, **8(47)**:13715–13719.
- [13] Del Sordo, S. et al. (2009). Progress in the development of CdTe and CdZnTe semiconductor radiation detectors for astrophysical and medical applications. *Sensors. Molecular Diversity Preservation International*, **9(5)**:3491–3526.
- [14] Tang, A. et al. (2010). Synthesis, optical properties, and superlattice structure of Cu (I)-doped CdS nanocrystals. *Applied Physics Letters. AIP*, **97(3)**:33112.
- [15] Tierney, J. and Lidström, P. (2009). Microwave assisted organic synthesis. John Wiley & Sons.
- [16] Tu, W. and Liu, H. (2000). Rapid synthesis of nanoscale colloidal metalclusters by microwave irradiation. *Journal of Materials Chemistry. The Royal Society of Chemistry*, **10(9)**:2207–2211.
- [17] Vohra, S. (2013). Synthesis and Characterization of PANI/PEANI Conducting Polymers-Au/Ag Nanoparticle Composites. Ph.D. thesis, Thapar University, Patiala- Punjab, India: 169 pp.
- [18] Wan, S. et al. (2004). Single-step synthesis of copper sulfide hollow spheres by a template interface reaction route. *Journal of Materials Chemistry*, **14(16)**: 2489-2491.
- [19] Yang, H.; Huang, C.; Su, X., and Tang, A. (2005). Microwave-assisted synthesis and luminescent properties of pure and doped ZnS nanoparticles. *Journal of Alloys and Compounds*, **402(1-2)**: 274-277.
- [20] Zeng, H.; Vanga, R. R.; Marynick, D. S. and Schelly, Z. A. (2008). Cluster precursors of uncapped CdS quantum dots via electroporation of synthetic liposomes. Experiments and theory. *The Journal of Physical Chemistry B*, **112(46)**: 14422-14426.
- [21] Zhang, A. Q. et al. (2014). pH-Dependent shape changes of water-soluble CdS nanoparticles. *Journal of nanoparticle research*, **16(1)**: 2197.
- [22] Mustafa, M. H. (2015). Effect of Annealing Temperature on the Structure and Optical Properties of CdS:Cu Thin Films Prepared By Thermal Vacuum Evaporation. *journal of the college of basic education*. **21(88)**:125–132.
- [23] Hao, Y.M. et al. (2012). Structural, optical, and magnetic studies of manganese-doped zinc oxide hierarchical microspheres by self-assembly of nanoparticle. *Nanoscale Research Letter*, **7(1)**:1-13.
- [24] Setvin, M.; Hulva, J.; Parkinson, G. S.; Schmid, M. and Diebold, U. (2017). Electron transfer between anatase TiO<sub>2</sub> and an O<sub>2</sub> molecule directly observed by atomic force microscopy. *Institute of Applied Physics*, **114(13)**:E2556–E2562.
- [25] J.V. Lauritsen et al. (2006). Chemical identification of point defects and adsorbates on a metal oxide surface by atomic force microscopy. *Nanotechnology*, **(17)14**:3436–3441.
- [26] Pentia, E.; Pintilie, L.; Pintilie, I. and Botila, T. (2000). The influence of cadmium salt anion on the growth mechanism and on the physical properties of CdS thin films. *Journal of Optoelectronics and Advanced Materials*, **(2)5**:593–601.

## توصيف أغشية كبريتيد الكاديوم الرقيقة المحضرة بطريقة التقطير الكيميائي

جمال مال الله رزيق ، سمير عبيد نواف ، محمد غازي حمد

قسم الفيزياء ، كلية العلوم ، جامعة الانبار ، رمادي ، العراق

### الملخص

باستخدام تقنية بسيطة تم إنماء أغشية كبريتيد الكاديوم (CdS) النانوية. تم تشكيل مسحوق من جسيمات نانوية كأغشية رقيقة باستخدام تقنية التقطير الكيميائي. أُدنت النماذج المحضرة عند درجة حرارة 200 °C ثم أُجريت فحوصات الأشعة السينية وطيف الأشعة فوق البنفسجية-المرئية وصور مجهر القوى الذرية إضافة إلى بعض خصائص العزل الكهربائي. أشارت النتائج إلى نقاوة عالية من أغشية CdS النانوية تم الحصول عليها بنجاح ذات تركيب بلوري سداسي الشكل بحجم 35nm باستخدام اتساع خط طيف الأشعة السينية. فجوة الطاقة البصرية للأغشية المحضرة والمعدنة تباينت ضمن المدى (3.35 - 3.73) eV. أظهرت نتائج مجهر القوى الذرية تجانسا في الحبيبات المترسبة بعد تلدينها بدرجة حرارة 200 °C وبمعدل خشونة للسطح بمقدار 3.83 nm. أفضل نتائج العزل الكهربائي تم الحصول عليها كانت للنماذج المعدنة.